RSC Advances

ROYAL SOCIETY OF CHEMISTRY

www.rsc.org/advances

Revised manuscript RA-ART-07-2014-006600

Targeting the heme proteins hemoglobin and myoglobin by janus green blue and study of the dye-protein association by spectroscopy and calorimetry†

Sabyasachi Chatterjee and Gopinatha Suresh Kumar*
Biophysical Chemistry Laboratory, Chemistry Division
CSIR-Indian Institute of Chemical Biology
Kolkata 700 032, India

Address for Correspondence:
Dr. G. Suresh Kumar
Senior Principal Scientist, Biophysical Chemistry Laboratory
CSIR-Indian Institute of Chemical Biology, 4, Raja S. C. Mullick Road
Kolkata 700 032, INDIA
Phone: +91 33 2472 4049 /2499 5723
Fax: +91 33 2473 0284 / 5197
e-mail: gskumar@iicb.res.in/gskumar@csiriicb.in

†Electronic supplementary information (ESI) available. See DOI:...

Revised manuscript RA-ART-07-2014-006600

Abstract

The binding of the phenazinium dye janus green blue (JGB) to two heme proteins, hemoglobin (Hb) and myoglobin (Mb), was studied by biophysical and microcalorimetry techniques. Ground state complex formation was ascertained from absorbance and fluorescence data. The binding affinity of JGB to myoglobin was higher than that to hemoglobin. The binding induced conformational changes in the proteins as revealed from circular dichroism, synchronous fluorescence and 3D fluorescence results. The binding was characterized in calorimetry by endothermic heats. The negative standard molar Gibbs energy in both cases suggested the spontaneity of the reaction. The positive enthalpy and positive entropy changes characterized the binding of the dye to both proteins. The higher affinity to Mb (K = 8.21×10^4 M^{-1}) over Hb (K = 6.60×10^4 M^{-1}) was confirmed from calorimetry results. The binding involved contribution from both polyelectrolytic and non-polyelectrolytic forces. pH dependent studies confirmed the involvement of ionic interactions in the complexation. The molecular details of the interaction in terms of structural aspects and energetics are described.

Revised manuscript RA-ART-07-2014-006600

Introduction

Hemoglobin and myoglobin are heme proteins whose main physiological function is to bind molecular oxygen. Hemoglobin (Hb) picks up oxygen from the tiny blood capillaries at the base of the lungs and carries it along the arteries to the body tissues, and also mopps up the H_3O^+ (aq) ions to control the acidity of the blood and carry CO_2 from the cells to the lungs to remove it. The enzymatic and antioxidant role of heme proteins are also well documented in the literature.[1, 2] Myoglobin (Mb) is found mainly in muscle tissues which receives oxygen from the red blood cells and transports it to the mitochondria of the muscle cells, where the oxygen is used in cellular respiration to generate energy.[3] Since hemoglobin and myoglobin bind oxygen it may be assumed that they have similarities in their structure and functions. Myoglobin is a single polypeptide chain protein of 153 amino acids with molecular weight 16.5 kDa. Hemoglobin, on the other hand, is a tetrameric protein of a molecular weight of 64.5 kDa comprising of four polypeptide chains: two identical α-chains comprising of 141 amino acid residues each and two identical β-chains made up of 146 amino acid residues. The α- and β-chains have different sequences of amino acids, but fold up to form similar three-dimensional structures. The four chains are held together by noncovalent interactions. The amino acids in Hb predominantly form α-helices which are interconnected by short non-helical segments. The helical sections inside Hb are mostly stabilized by hydrogen bonding interactions which results in attractions within the molecule leading to the folding of the polypeptide chains into a particular shape.

Revised manuscript RA-ART-07-2014-006600

The polypeptide chain of Mb comprises of eight separate right handed α-helices, designated A through H, that are connected by short non-helical regions. Amino acid R-groups, packed into the interior of the molecule, are predominantly hydrophobic in character while those exposed on the surface of the molecule are generally hydrophilic thus making the molecule relatively water soluble. Its secondary structure contains a very high proportion (~75%) of α-helices. Neither Hb nor Mb contain disulphide bonds.[4]

It is known that the distribution of biologically active compounds *in vivo*, including drugs, natural products and toxic materials, are based on their affinity to the plasma proteins. Although Hb and Mb are not strictly plasma proteins Hb will be available in the plasma on hemolysis. Therefore, investigations on the interaction of drugs, dyes and toxic small molecules with hemoglobin are of great importance in terms of understanding their pharmacological actions. Recently, a number of studies on small molecules binding to Hb have been reported [5-15] while studies on the binding of small molecules to Mb are scarse[16-19].

Janus green B (JGB) (3-(diethylamino-7-(4 113 dimethyl amino phenyl azo)-5-phenylphenazinium chloride) (Fig. 1) is a basic phenazinium dye having anti malarial potency[20] and known to behave as an accurate inhibitor for specific supravital staining of mitochondria.[21,22] It is also used for the quantification of trace amount of adverse pollutants like thiourea and formaldehyde in industrial waste water samples.[23] DNA binding studies of this dye have been reported.[24] Binding to double stranded polyadenylic acid was found to involve intercalation.[25]

Revised manuscript RA-ART-07-2014-006600

Studying the binding mechanism to heme proteins by evaluating the binding parameters, binding sites and the associated energetics is critical for understanding the pharmacodynamics, pharmacokinetics, distribution, and potential interference leading to effective drug availability, sequestration etc.[26] Traditionally most of the drug molecules are cationic species and may contain aromatic conjugated systems. Here we elucidate the comparative binding ability of the cationic dye, janus green blue, to two heme proteins as a model system from a variety of biophysical techniques. Thermodynamics of the interaction has also been elucidated to correlate with the structural data.

Results and discussion

Absorption spectral study

The UV–vis absorption spectroscopy technique was used to explore the interaction of the dye with the proteins. The absorption spectrum of Hb has two major peaks in the 190–600 nm regions with maxima at 195 nm and 405 nm, respectively, shown in the Fig. 2A. The former peak is mainly due to the π-π* transitions of the carbonyl (C=O) groups of the amino acid residues and the latter is from the porphyrin-Soret band (π-π* transition).[13] The Soret band originates from the heme group embedded in a hydrophobic pocket formed by the protein's backbone through appropriate folding.[27] The absorption spectrum of Mb (Fig. 2B) in the 250-700 nm region also exhibited two prominent peaks, one at 280 nm (for tryptophans and tyrosines) and one at 408 nm (the heme soret band), followed by a less intense one at 504 nm (the Q band).

Revised manuscript RA-ART-07-2014-006600

In the presence of increasing concentration of JGB there was a significant decrease in the absorbance of both proteins as shown in the Fig. 2. The contribution of JGB to the total absorbance was nullified with the presence of equivalent amount in the reference cuvette. This result indicated that a ground state complex formation is occurring between the proteins and the dye.[28] Isosbestic points at 231, 378 and 423 nm for Hb, and 299 and 345 nm for Mb were observed in the series of spectra. In the inset of Fig. 2A and 2B the changes in the 195 and 405 nm peaks for Hb and 408 nm peak for Mb were amplified and presented. It can be observed that there is a small blue shift (2 nm) in the 195 nm band of Hb in the presence of JGB. The behaviour of the Soret band, however, was similar in both the cases and showed only a decrease in the absorbance.

The effect of the proteins on the absorption spectrum of JGB was also performed and the same is depicted in Fig. 3. JGB has an absorbance maximum at 600 nm in the range of 500-800 nm that was found to undergo a hypochromic effect with gradual addition of both proteins. There was a blue shift 8 nm for the band in the presence of Hb shown in the Fig. 3A. On the other hand, a remarkably large blue shift of the peak maximum by about 40 nm was observed in the case of Mb as shown in the Fig. 3B. Additionally, in the case of Mb the band was split into two parts at high dye concentrations and such a behaviour was not observed with Hb. The protein induced spectral changes may be rationalized in terms of a lowering in the polarity of the immediate environment around the dye, being very high in the presence of Mb.[29] The spectral titration data were analysed by Benesi-Hildebrand plot to determine the equilibrium constants using the following relation[30]

Revised manuscript RA-ART-07-2014-006600

$$\frac{1}{\Delta A} = \frac{1}{\Delta A_{max}} + \frac{1}{K_{BH}(\Delta A_{max})} x \frac{1}{[M]} \quad (4)$$

where, A is the absorbance, K_{BH} is the Benesi-Hildebrand binding constant and [M] is the concentration of the dye. A plot of $1/\Delta A$ against $[M]^{-1}$ gave straight lines in both cases, thereby, justifying the validity of the above equation and hence confirming one to one interaction between the dye and the proteins. The binding affinity values obtained from the analysis were 8.60 x 10^4 M^{-1} and 10.14 x 10^4 M^{-1}, respectively, for Hb and Mb. The magnitude of the K_{BH} values suggest that JGB has a higher affinity to Mb than Hb.

Steady state fluorescence spectral study

Fluorescence spectroscopy is a powerful and rich technique to characterize the interaction and also to gain access to the environment of the fluorophore in the protein matrix. This is very useful for justification of both dipole-orientation dynamics of molecules surrounding the chromophore and their dielectric properties and plays a crucial role in charactering the microenvironment of protein. Detailed information like binding affinity, binding sites, dynamics and conformational transformations can also be derived from fluorescence studies. The intrinsic fluorescence of Hb and Mb arise essentially from the tryptophan (Trp) and tyrosine (Tyr) residues present in the polypeptide chain, and these residues are very sensitivities to their microenvironment. Therefore, we took advantage of fluorescence spectroscopy to investigate the interaction between the proteins and the dye. It is previously known that the emission maximum of tryptophans is more sensitive to the local environment than that of the tyrosines. To understand the effect of JGB complexation on the proteins, the fluorescence emission spectra of the

Revised manuscript RA-ART-07-2014-006600

proteins were monitored by exciting at 295 nm exciting selectively the Trp residues.[31] Both Hb and Mb showed emission maxima at 328 nm, the intensity of which gradually decreased with increasing JGB concentration. This data is presented in Fig. 4. Shift in the peak position was not observed in either case. This result reveled that the dye interacted with the proteins and the fluorescence quenching was due to specific complex formation.

Temperature dependent fluorescence spectral study

The quenching of the protein fluorescence by a small molecule may be either due to static or dynamic quenching. Static quenching is usually due to the ground-state complex formation between the protein and the small molecule. Increasing the temperature will decrease the Stern–Volmer quenching constant (K_{SV}) due to decreasing stability of the protein-dye complex in the case of ground state complexes. In contrast, dynamic quenching essentially results from collision between the protein and the dye.

Both static and dynamic quenching processes are described by the Stern–Volmer equation,

$$\frac{F_0}{F} = 1 + Kq\,\tau_0[Q] = 1 + K_{SV}[Q] \qquad (5)$$

where, F_0 and F are the steady-state fluorescence intensities in the absence and in the presence of the quencher (JGB here), K_q is the quenching rate constant, τ_o represents the average fluorescence lifetime, K_{SV} is the Stern–Volmer quenching constant and [Q] is the concentration of the quencher. The possible quenching mechanism of JGB–protein complex formation can be elucidated from the fluorescence quenching spectra of protein-dye complexes following Stern–Volmer plots at different

Revised manuscript RA-ART-07-2014-006600

temperatures. Figure 5 shows the Stern–Volmer plots of F/F_0 versus [Q] at the three temperatures for JGB complexes with the proteins. The calculated K_{SV} and K_q values are summarized in Table 1. In both cases the K_{SV} values decreased with increasing temperature, suggesting weakening of the protein-JGB complexes. The result testifies that the fluorescence quenching in both proteins induced by the dye is due to complex formation and not by dynamic collision. In other words, the quenching of the fluorescence of the proteins by JGB is due to specific complex formation and dynamic collision effects, if any, may be negligible. This confirms the presumption of ground state complexation inferred from the absorbance spectral data.

Now that the complex formation is established, for the static quenching mechanism, if it is assumed that there are independent binding sites to a set of equivalent sites on the protein, the apparent binding constant and the number of binding sites can be determined from the following equation,

$$\log \frac{(Fo - F)}{F} = \log K_A + n \log[Q] \qquad (6)$$

where K_A is the binding constant to a site and n is the number of binding sites per protein. From the linear plots of log (F_0-F/F) versus log [Q] (Fig. S1†) the binding affinity values of JGB binding to the proteins were obtained at the three temperatures. These data are presented in Table 1. The 'n' values were found to be around one, suggesting one binding site for these dyes around the Trp residues of the proteins.

The quenching data were also analyzed by employing the Lineweaver–Burk equation,

Revised manuscript RA-ART-07-2014-006600

$$\frac{1}{(F_O - F)} = \frac{1}{F_O} + \frac{1}{K_{LB} F_O [Q]} \qquad (7)$$

where the static quenching constants (K_{LB}) were obtained from the ratio of the intercept to the slope of the Lineweaver–Burk plot, describing the efficiency of quenching at the ground state. The data depicted in Table 1 revealed that the value is higher for Mb than Hb complex. The K_{LB} values were found to decrease with the temperature. The decreasing trend in K_{LB} values with increasing temperature for the complexes was, again, in accordance with the temperature dependence of K_{sv} values and is consistent with a static quenching mechanism.

Synchronous fluorescence spectroscopy

Synchronous fluorescence spectroscopy is a technique introduced by Lloyd[32] and used extensively for characterising small molecules binding to proteins.[6,13,14,33] It involves simultaneous scanning of the excitation and emission monochromators maintaining a constant wavelength interval between them. The synchronous fluorescence spectroscopy gives information about the molecular environment in a vicinity of the chromophore molecules. This technique has several advantages, like high sensitivity, spectral simplification, spectral bandwidth reduction and avoidance of different perturbing effects.

The synchronous fluorescence spectra of Hb and Mb contributing from the Tyr and Trp residues were obtained by a simultaneous scanning of the excitation and emission wavelength in the 15 band 60 nm wavelength intervals.[34] For the synchronous fluorescence spectra of protein, when the $\Delta\lambda$ value between the excitation and emission wavelengths was 15 nm or 60 nm, respectively, gives characteristic information about change in Trp and Tyr residues due to the presence

Revised manuscript RA-ART-07-2014-006600

of the bound dye molecules. The synchronous fluorescence spectra of Hb and Mb in the presence of different concentration of dye molecule are shown in Fig. 6. It can be seen that the fluorescence intensities of both Hb and Mb decreased regularly with increasing concentration of JGB. For Δλ=60 nm a small red shift of peak maxima of 6 nm was observed in case of Hb but in Mb 3 nm blue shift was observed. The red shift is indicating that the conformation of proteins was changed, the polarity around the Try residue was increased and hydrophobacity decreased and in blue shift reverse polarity around Tyr was observed. In the Mb there is a negligible transformation in the microenvironment around the Try. In the of Hb there was a red shift of 8 nm of the emission maximum when Δλ was set at 15 nm, showing that the polarity around Try residue was increased and hydrophobacity was decreased. But in the case of Mb there was a 5 nm blue shift in synchronous fluorescence.

Circular dichroism spectroscopy

Circular dichroism (CD) is a spectroscopic technique widely used for the measurement of the conformation and stability of proteins in several environmental conditions and in the presence of different small molecules including change in secondary and tertiary structures. CD probes the secondary structure of proteins because the peptide bond is asymmetric and molecules without a plain of symmetry exhibit circular dichroism.

Far-UV CD is a powerful analytical technique to study of molecular assembly of proteins with other small molecules, and to determine the change in protein conformational change and inter conversion between the conformations. In the far-UV CD (range of 250-190 nm) the native Hb and Mb exhibited two negative peaks

Revised manuscript RA-ART-07-2014-006600

centred at 208 nm and 222 nm, characteristic of the α-helical structure of the globular proteins, originating from the n→π* transition for the peptide bond of the α-helix.[35] In both the cases the band intensity of these bands decreased in the presence of JGB (Fig. 7A, C). This indicated the loss of α-helicity upon interaction with the dye. In the case of Hb no significant shift of the peaks was observed, but in Mb there is red shift (about 3 nm) for the 222 nm band. In comparison to Hb, the change in CD band for Mb was much lower due to dye binding. So Mb appears to retain its secondary structure on binding of the dye molecule compared to the other protein.

The Soret band arises from an electron dipole movement that allows π-π* transition; common in porphyrin compounds.[36] The Soret band of the CD spectrum is important to understand the change in nature of porphyrin ring due to the binding of small molecule. In the Soret region, both Hb and Mb exhibited a complex circular dichroism with a large positive maximum and a small negative trough as shown in the Fig.7 B,D. The position of the maxima was slightly different for the two proteins; 408 nm for Hb and 413 nm Mb. The intensity of the band decreased in both cases with gradual increase of the dye concentration. This revealed that in both cases the planarity of the porphyrin ring was changed upon binding of the dye molecule.

To examine the conformational aspects in more detail, induced CD spectra were recorded in the region of 500-700 nm where neither the proteins nor JGB has any CD spectra, the dye being an achiral molecule. But gradual addition of Mb solution to the dye generated a CD band that increased in ellipticity with maximum at 600 nm near the absorbance maximum of JGB (Fig. 8A). But, surprisingly, no induced CD bands were generated in case of Hb under identical experimental condition (Fig. 8B).

Revised manuscript RA-ART-07-2014-006600

Though JGB is achiral a CD signal was induced because it may be bound in an asymmetric fashion in the chiral environment of Mb and interaction of the transition moments of the dye and the amino acid residues of the protein induced optical activity in the dye. The orientation of the dye in Hb, therefore, appears to be different leading to nullification of the transition moments of the dye and the protein residues and hence no induced CD was generated.

Conformational investigation by three-dimensional fluorescence

Three-dimensional fluorescence spectroscopy is a new analytical technique that is applied to investigate conformational changes in proteins.[37,38] The excitation and emission wavelengths of the fluorescence intensity can be used as the axes rendering the investigation of the characteristic conformational changes of proteins more scientific and credible. The maximum fluorescence emission wavelength of amino acid residues in a protein is related to the polarity of the environment and fluorescence emission spectrum wavelength and the synchronous fluorescence spectrum wavelength of heme proteins in the absence and presence of dye may show distinct differences and sharp changes providing relative information on the configuration of the protein. The three-dimensional spectra and contour maps of the complexes Mb and HB with JGB are presented in Fig. 9 and the data are depicted in the Table S1†. In the three dimensional spectra, two representative fluorescence peaks (peak 1 and peak 2) were clearly observed, peak a and peak b represents Rayleigh scattering peak (λex = λem) and second-order scattering peak (λem = 2λex), respectively, these peaks indicated that the binding of the dye causes conformational changes in heme proteins leading to quenching . Since the proteins are excited at 280

Revised manuscript RA-ART-07-2014-006600

nm it reveals the intrinsic fluorescence of Trp and Tyr residues, and negligible fluorescence of the Phe residues we suppose that peak 1 is characteristic for Trp and Tyr and peak 2 perhaps represents for polypeptide backbone structures.

Thermodynamics of the interaction

Isothermal titration calorimetry (ITC) is a valuable method for characterising the energetics of molecular interaction. Presently ITC is the only technique that directly measures the binding enthalpy and stoichiometry with high accuracy with the additional advantage of providing the binding affinity and stoichiometry from a single titration.[39,40] Moreover, ITC data allows dissection of the Gibbs energy of binding into enthalpic and entropic components, revealing the overall nature of the forces that drive the binding interaction.

In Fig. 10, the data from the calorimetric titration of JGB to Hb and Mb at 20 °C are presented. Each heat burst curve in the figure corresponds to a single injection. These heats were corrected by subtracting the corresponding dilution heats obtained from control experiments of injecting identical amounts of the dye solutions into the buffer alone (shown at the top portion of the upper panels, curves offset for clarity). In the bottom panels of the figure, the resulting corrected heats of the complexation are plotted against the molar ratio. The binding was characterized by endothermic heats in each case characteristic of hydrogen bond interactions and conformational changes. The data points in the lower panels are the experimental points and the continuous lines are the calculated best fit of the data to the model. Since there was only one binding event in the titration data (upper panel) a single set of binding model with lowest $\chi 2$ value was used for the analysis. The results of the ITC

Revised manuscript RA-ART-07-2014-006600

experiments are presented in (Table 2). It can be seen that the affinity of JGB to Mb was higher (K=8.21×10^4 M^{-1}) than that to Hb (K=6.60×10^4 M^{-1}). The stoichiometry was around 1.0 confirming the observations from the fluorescence data. The thermodynamic data suggests that the complexation was spontaneous and entropy driven with a favourable enthalpy contribution to the Gibbs free energy. The large entropy contribution suggests significant conformational changes and changes in water structure on binding.

pH dependent fluorescence study: Role of electrostatic interactions

It is known that ionisable amino acid residues have remarkable influence on protein structure, stability and solubility, and have been shown to influence the binding of small molecules.[41,42] Therefore, the nature and type of interactions that control and regulate the ligand-protein binding may, essentially, depend on the pH of the medium. We, therefore, investigated the influence of pH on the binding of JGB to Hb and Mb from fluorescence studies. The steady state fluorescence emission studies were performed on both proteins by exciting at 295 nm in the presence of JGB at three different pH, 6.4, 7.4, and 8.4 monitoring the emission maxima at 329 nm. The results were analyzed by Stern-Volmer plots shown (Fig. 11) and the data are presented in Table S2†. It can be observed that the K_{sv} values were maximum at pH 6.4 and decreased with increasing pH for both proteins. This result suggests the existence of strong electrostatic interactions between the protein molecules and the dye.[43]

Melting Experiments

A: UV-melting study

Revised manuscript RA-ART-07-2014-006600

Evidence for the interaction of JGB to the proteins was also obtained from the measurement of UV-thermal melting experiment. Under the conditions of the experiment both Hb and Mb exhibited a sharp melting transition with melting temperatures around 59.5 and 82.57 ^{0}C, respectively. Under the saturation condition (D/P =2.0) the thermal melting temperatures were shifted 51.58 and 70.95 ^{0}C, respectively, for Hb and Mb. So JGB destabilized Hb and Mb by 7.92 and 11.62 ^{0}C, respectively, due to complexation as shown in the Fig. 12 A, C. The higher destabilization of Mb was thus evident from these studies.

B: CD melting study

Thermal stability of the proteins upon binding of the dye molecule was monitored by circular dichroism spectroscopy by following spectral changes with increasing temperature. A single wavelength can be chosen which monitors some specific feature of the protein structure, and the signal at that wavelength is then recorded continuously as the temperature is raised. We monitored the changes at the 222 nm, the peak minima in the far-UV-CD spectra in both Hb and Mb to realize the CD melting in the temperature range 25 to 110 ^{0}C. The CD-melting experiment of proteins was performed with the native form and complex (D/P =2.0) separately. The melting temperatures of uncomplexed Hb and Mb were 60.01 and 81.61 ^{o}C, respectively. Upon complexation with the dye the melting temperature (T_m) was shifted to 52.88 and 71.09 ^{o}C, respectively, as shown in the Fig. 12, B and D. This result reveled that due to complexation the stability of the proteins decreased and difference of melting temperature (ΔT_m) was 7.13 and 10.52^{o}C, respectively, for Hb

Revised manuscript RA-ART-07-2014-006600

and Mb. The results are in agreement with those obtained from absorbance melting. So JGB destabilized Mb more than Hb upon complexation.

Conclusions

Here we present a series of spectroscopic and calorimetric experiments to understand the binding aspect of the phenazinium dye janus green blue to two heme proteins hemoglobin and myoglobin. JGB is a positively charged dye useful in many biological applications. The results of this study revealed that JGB binds more strongly to the single polypeptide chain Mb compared to the tetrameric Hb although the binding to both proteins followed a 1:1 stoichiometry. The binding induced quenching of the protein fluorescence was characterized to be due to the formation of specific complexes at the ground state. Significant conformational changes were induced in the proteins on binding of the dye as revealed from synchronous and 3D fluorescence, and CD spectra, but there were differences in the generation of induced CD, reiterating stronger binding of the dye to Mb.

Thermodynamic parameters obtained from isothermal titration calorimetry suggested that the binding was favoured by both negative enthalpy and strong favourable entropy contributions with both BSA and HSA. For the charged alkaloid electrostatic interactions may be the dominant force in binding. This notion was strengthened from the fact that there is significant enthalpic component for the binding indicating forces other than hydrophobic effect also contributes significantly to the binding that must be electrostatic, van der Waals and H-bonding interactions. Furthermore, the pH dependent studies also confirmed the role of charged side

Revised manuscript RA-ART-07-2014-006600

chains in the complexation. Overall, the binding of the dye to Mb was stronger and favoured more than that to Hb.

Materials and methods

Materials

Human hemoglobin, equine skeletal muscle myoglobin and the dye janus green blue were obtained from Sigma-Aldrich Corporation (St. Louis, MO, USA). The proteins were purified as reported earlier.[14] Janus green blue (CAS No. 2869-83-2, colour index no. 1105) was recrystallised from alcohol and dried in a desiccator at 40 ^{0}C. The samples were prepared in sodium phosphate buffer (10 mM Na^+) of pH 7.2. pH measurements were made on a Sartorius PB-11 high precision bench pH meter (Sartorius GmBH, Germany) with an accuracy of > ±0.01. The concentrations were determined by absorption spectral measurement using molar absorption coefficient (ε) values of 17,900 M^{-1} cm^{-1} at 405 nm for Hb, 17,900 M^{-1} cm^{-1} at 408 nm for Mb and 38,000 M^{-1} cm^{-1} at 600 nm for JGB.[44,45] No deviation from Beer's law was observed for the dye in the concentration range used in this study. All chemicals and reagents used in this study were of analytical grade and obtained from Sigma-Aldrich. Glass distilled and deionised water was used for buffer preparation. The buffer solution was filtered through Millipore filters (Millipore India Pvt. Ltd, Bangalore, India) of 0.22 μm pore size before use.

The JGB solution was freshly prepared each day in the experimental buffer and kept protected in the dark to prevent any photochemical changes due to exposure to light. The overall JGB concentration in each experiment was keep at the lowest possible level to prevent aggregate formation and minimise the inner filter effects.

Revised manuscript RA-ART-07-2014-006600

Methods

Electronic absorption spectroscopy

The absorption spectral titrations were performed at 20± 0.5 ^{0}C on a Jasco V660 spectrophotometer (Jasco International Co. Ltd., Hachioji, Japan) equipped with a thermoelectrically controlled cell holder and temperature controller in matched quartz cuvettes of 1 cm path length. In dye-protein studies after each addition of an aliquot of the dye to the protein solution, the solution was thoroughly mixed and allowed to re-equilibrate for at least 5 min. before noting the absorbance values at the desired wavelength maxima.

Fluorescence spectroscopy

Steady state fluorescence, synchronous fluorescence and pH dependent fluorescence spectra were measured at 20±0.5 ^{o}C on a Shimadzu RF-5301PC spectrofluorophometer (Shimadzu Corporation, Kyoto, Japan). Temperature dependent fluorescence experiments were performed on a Hitachi F4010 (Hitachi Ltd., Tokyo, Japan) fluorescence spectrometer attached with Eylea Uni Cool U55 water bath (Tokyo Rikakikai Co. Ltd., Tokyo, Japan) to control the temperature of the cuvette. The temperature was monitored by the electronic devise Sensortek, model BAT-12 Microprobe Thermometer (Sensortek Inc., New Jersey, USA). All the fluorescence measurements employed 1 cm path length fluorescence free quartz cuvettes (Hellma, Germany).

For measurements of intrinsic fluorescence of Hb and Mb in the presence of JGB, the protein samples were excited at 295 nm, the excitation maximum of tryptophan and the emission spectra scanned in the range 300 to 500 nm. For measurement of

Revised manuscript RA-ART-07-2014-006600

synchronous fluorescence the excitation wavelength was set as 220 nm and Δλ was set at 60 and 15 nm, respectively, for tryptophan and tyrosine moieties.

The fluorescence emission intensities of Hb and Hb-complexes were always corrected for inner filter effect due to the strong absorption of heme protein and the dye in the UV−vis region as detailed previously.[14]

Three-dimensional fluorescence studies

Three-dimensional (3D) fluorescence spectroscopy experiments were performed at 20 ± 0.5 ^{0}C on a PerkinElmer LS55 fluorescence spectrometer (PerkinElmer Inc., USA). The fluorescence emission spectra of Hb and Mb were measured in the range 270–500 nm with an increment of 10 nm; the initial excitation wavelength was set at 200 nm and continued up to 340 nm, i.e., the number of scans was 15. The concentration of Hb and Mb were 5 μM each and the protein: dye complex ratio was set 1:6 in both cases.

Circular dichroism measurements

A Jasco J815 spectropolarimeter (Jasco International Co., Ltd.,) equipped with a Peltier controlled cell holder and temperature controller PFD 425 L/15 was used for monitoring the conformational changes in the proteins on binding of JGB as reported in earlier studies.[14] The protein concentration and path length of the cuvettes used were 1.0 μM and 0.1 cm, respectively, for far-UV CD region and CD 5.0 μM and 1 cm, respectively for the Soret band. The instrument parameters for CD measurements were set as follows: scanning speed 50 nm/min., bandwidth of 1.0 nm, and sensitivity of 100 milli degrees. A buffer baseline scan was subtracted from the averaged scan for each sample. Ten scans were averaged and smoothed to

Revised manuscript RA-ART-07-2014-006600

improve signal-to-noise ratio. The titration experiments were performed at 20 ^{0}C. The molar ellipticity value [θ] (deg cm^2 dmol^{-1}) are calculated from the equation

$$MRE[\theta]_\lambda = \frac{observedCD(m\,deg)}{Cnl \times 10} \qquad (1)$$

where [θ] is the observed ellipticity (milli degree), C is the molar concentration, *n* is the number of amino acid, n is the number of amino acid residues and l is the optical path length of the cuvette (cm) and residues. The molar ellipticity value of CD was expressed in terms of the mean residue molar ellipticity [θ], in units of deg cm^2 dmol^{-1}.

Isothermal titration calorimetry

The energetics of the binding of JGB to Hb and Mb was studied by isothermal titration calorimetry (ITC) using a MicroCal VP-ITC unit (MicroCal, LLC, Northampton, MA, USA) following the protocols developed in our laboratory and described in details elsewhere.[13] The proteins and dye solutions were thoroughly degassed on the MicroCal's Thermovac unit before loading to avoid air bubble formation during the course of the titration. The instrument control, titration and data analysis were performed by the dedicated Origin 7.0 software of the calorimeter. The calorimeter syringe was filled with a solution of JGB (500 μM for titration with Hb and 1000 μM for Mb). Successive injections of 10 μL aliquots of the dye solution into the Hb (50 μM) and Mb (20 μM) solutions contained in the calorimeter cell (capacity 1.4235 mL) were programmed to be effected from the rotating syringe (416 rpm). Heats of dilution for the dye were determined in control experiments, and these were subtracted from the integrated data before curve fitting. The area under each heat burst curve was determined by integration using the

Revised manuscript RA-ART-07-2014-006600

Origin software to give the measure of the heat associated with the injections. The resulting corrected injection heats were plotted as a function of the molar ratio, fit with a model for one set of binding sites and analyzed to provide the binding affinity (K), the binding stoichiometry (N), and the standard molar enthalpy of binding ($\Delta H°$). The standard molar Gibbs energy ($\Delta G°$) and the entropy contribution to the binding ($T\Delta S°$) were subsequently calculated by the following equations

$$\Delta G^o = -RT \ln K \qquad (2)$$

and

$$\Delta G^o = \Delta H^o - T\Delta S^o \qquad (3)$$

where T is the temperature in kelvin and R is the universal gas constant (1.9872041 cal mol^{-1} K^{-1}). Periodic calibration of the calorimeter was performed as per the criteria of the manufacturer that the mean energy per injection was ≤1.30 µcal and standard deviation was ≤0.015 µcal.

Optical melting studies: UV- thermal melting

Absorbance versus temperature curves (melting profiles) of Hb and Mb, and the protein-dye complexes were measured on the Shimadzu Pharmaspec 1700 unit (Shimadzu Corporation) equipped with the Peltier controlled TMSPC-8 model cuvette accessory. In a typical experiment, protein sample (5 µM) was mixed with different concentrations of the JGB in the degassed buffer and transferred into the eight chambered micro cuvette of 1 cm path length (100 µL) and the temperature of the microcell accessory was raised at a heating rate of 0.5 °C/min, continuously monitoring the absorbance change at 295 nm scaning in the temperature range 20 to

Revised manuscript RA-ART-07-2014-006600

110 ^{0}C. The melting temperature (T_m) was taken as the midpoint of the melting transition as determined by the maxima of the first derivative plots.

Circular dichroism melting

The thermal denaturation experiments in circular dichroism were carried between 20-110 °C with at a scan rate of 0.5 °C /min. monitoring the change in ellipticity at 222 nm. The curves were normalized, assuming a linear temperature dependence of the base lines on native and denatured states.

Acknowledgements

Financial assistance for this work from the project BIOCERAM (ESC 0103) of the Council of Scientific and Industrial research (CSIR) is acknowledged. S. C. is supported by the Junior Research Fellowship of the University Grants Commission, Government of India awarded through NET. The authors thank all the colleagues of the Biophysical Chemistry Laboratory for their help and support during the course of this work. The critical and helpful comments by the anonymous referees that enabled us to improve the manuscript are also gratefully acknowledged.

References

1. R. Mandal, R. Kalke and X. F. Li, *Chem. Res. Toxicol.*, 2004, **17**, 1391–1397.
2. L. Messori, C. Gabbianii, A. Casini, M. Siragusa, F. F. Vincieri and A. R. Bilia, *Bioorg. Med. Chem.*, 2006, **14**, 2972–2977.
3. M. M. Cox and G. N. Phillips Jr., *Handbook of Proteins: Structure, Function and Methods*, Wiley, West Sussex, 2007.
4. J. A. Lukin and C. Ho, *Chem. Rev.*, 2004, **104**, 1219–1230.
5. P. Mandal, M. Bardhan and T. Ganguly, *J. Photochem. Photobiol. B*, 2010, **99**, 78–86.
6. W. Liu, F. Ding and Y. Sun, *J. Solution Chem.*, 2011, **40**, 231-246.

Revised manuscript RA-ART-07-2014-006600

7. H. Cheng, H. Liu, W. Bao and G. Zou, *J. Photochem. Photobiol. B*, 2011 ,**105,** 126-132.
8. S. Chakraborty, S. Chaudhuri, B. Pahari, J. Taylor, P. K. Sengupta and B. Sengupta, *J. Lumin.*, 2012, **132,** 1522–1528.
9. Y.Q. Wang and H.M. Zhang , *J. Photochem. Photobiol. B*, 2012 ,**113**,14-21.
10. B. Sengupta , S. Chakraborty , M. Crawford, J.M. Taylor , L.E. Blackmon , P.K. Biswas and W.H. Kramer, *Int. J. Biol. Macromol.*, 2012, **51**, 250– 258.
11. Y. Liu, J. Lin, M. Chen and L. Song, *Food Chem. Toxicol.*, 2013,**58**, 264-272.
12. A.H. Hegde, B. Sandhya and J. Seetharamappa, *Int. J. Biol. Macromol.*, 2013, **52**,133–138.
13. S. Hazra and G. Suresh Kumar, *Mol. BioSyst.*, 2013, **9**, 143—153.
14. S. Hazra and G. Suresh Kumar, *J. Phys. Chem. B*, 2014, **118** , 3771–3784.
15. W. Peng, F. Ding, Y.-K. Peng and Y. Sun, *Mol. BioSyst.*, 2014, **10**, 138—148.
16. P. Taboada, Y. Fernández and V. Mosquera, *Biomacromolecules*, 2004, **5**, 2201–2211.
17. P. Mandal, M. Bardhan and T. Ganguly, *Luminescence*, 2012, **27**, 285-91.
18. M. G. I. Galinato , R. S. Fogle III and J. F. Galan, *Spectrochim. Acta, Part A*, 2013, **115**, 337–344.
19. X. He and Z. Song, *Spectrochim. Acta, Part A*, 2013, **114**, 231–235.
20. J.L. Vennerstorm, M.T. Makler, C.K. Angerhofer and J.A. Williams, *Antimicrob. Agents Chemother.*, 1995, **39**, 2671–2677.
21. A. Kruszewska and B. Szczesniak, *Mol. Gen. Genet.*, 1978, **160**, 171–181.
22. J. Ding, L. Zhang, F. Qu, X. Ren, X. Zhao, Q. Liu, *Electrophoresis*, 2011, **32**, 455-579.
23. S. Abbasi, M. Esfandyarpour, M.A. Taher and A. Daneshfar, *Spectrochim. Acta, Part A*, 2007, **67**, 578–581.
24. C. Z. Huang, Y. F. Li, X. H. Huang and M. Li, *Analyst*, 2000, **125**, 1267–1272.
25. A. Y. Khan , B. Saha and G. Suresh Kumar, *Spectrochim Acta, Part A*, 2014, **131**, 615-624.

Revised manuscript RA-ART-07-2014-006600

26. T. Khazaeinia, A. A Ramsey and Y. K. Tam, *J. Pharm. Pharm. Sci*., 2000, **3**, 292−302.
27. E.F. Nassar, J.F. Rusling and N. Nakashima, *J. Am. Chem. Soc*., 1996, **118**, 3043–3044.
28. R.E. Kay, E.R. Walwick and C.K. Gifford, *J. Phys. Chem*., 1964, **68**, 1907–1916.
29. M. Shannigrahi, R. Pramanik and S. Bagchi, *Spectrochim. Acta, Part A*, 2003, **59**, 2921–2933.
30. M.L. Benesi and J.H. Hildebrand, *J. Am. Chem. Soc*., 1949, **71**, 2703–2707.
31. J. R. Lakowicz, *Principles of Fluorescence Spectroscopy,* Plenum Press, New York,1983.
32. J.B.F. Lloyd, *Nature*, 1971, **231**, 64–68.
33. C. Jash and G. Suresh Kumar, *RSC Adv.,* 2014, **4**, 12514–12525.
34. Y.Q. Wang, H.M. Zhang, G.C. Zhang, S.X. Liu, Q.H. Zhou, Z.H. Fei and Z.T. Liu, *Int. J. Biol. Macromol*., 2007, **41**, 243–250.
35. N. J. Greenfield, *Nat. Protocols*, 2006, **1**, 2876–2890.
36. M. Nagai, Y. Sugita and Y. Yoneyama, *J. Biol. Chem*., 1969, **244**, 1651-1653.
37. Y. Qian, X. Zhou, J. Chen and Y. Zhang, *Molecules*, 2012, **17**, 6821-6831
38. A. Das and G. Suresh Kumar, *RSC Adv.*, 2014, **4**, 33082-33090 .
39. M. S. Celej, S. A. Dassie, E. Freire, M. L. Bianconi and G. D. Fidelio, *Biochim. Biophys. Acta***,** 2005, **1750**, 122–133.
40. Y. Liang, *Acta Biochim Biophys Sin*, 2008, **40**, 565-576.
41. G. R. Grimsley, J. M. Scholtz and C.N. Pace, *Protein Sci*., 2009, **18**, 247–251.
42. P. Kukic´, D. Farrell, C.R. Sondergaard, U. Bjarnadottir and J. Bradley,*Proteins*, 2010, **78**, 971–984.
43. N.V. Di Russo, D. A. Estrin, M. A. Marti and A. E. Roitberg, *PLoS Comput. Biol*., 2012, 8, e1002761.
44. E. Antonini and M. Brunori, Hemoglobin and Myoglobin in their Reactions with Ligands, North-Holland publishing Co., Amsterdam,The Netherlands, 1971.

Revised manuscript RA-ART-07-2014-006600

45. H.E. Johansson, M.K. Johansson, A.C. Wong, E.S. Armstrong, E.J. Peterson, R.E.Grant, M.A. Roy, M.V. Reddington and R.M. Cook, *Appl. Environ. Microbiol*. 2011, **77**, 4223–4225.

Revised manuscript RA-ART-07-2014-006600

Legends of Figures

Fig. 1: Chemical structure of janus green blue.

Fig. 2: Absorption spectral changes of heme proteins in the presence of JGB. (A) Hb (3.5 µM) treated with 29 µM of JGB. (B) Mb (8 µM) treated with 60 µM of JGB. Inset: (A) 195 nm and 405 nm bands of Hb (3.5 µM) treated with 0, 2.56, 6.72, 17.6 and 29 µM (curves 1−5) of JGB and(B) 409 nm bands of Mb (8 µM) treated with 0, 6,17,43 and 60 µM (curves 1−5) of JGB are highlighted.

Fig. 3: Absorption spectral changes of JGB in the presence and absence of the heme proteins. (A) JGB of 5.6 µM treated with 0, 0.7, 2.1, 3.5, 5.6, 7.7, 10.5, 12 and 14 µM of Hb (curves 1−9) and (B) JGB of 10.36 µM treated with 0, 2.9, 6.8, 9.8, 12.8, 22.8, 31.8, 58.8 and 65.8 µM of Mb (curves 1−9). (C) and (D) represnet the Benesi-Hildebrand plots for the binding of JGB with Hb and Mb.

Fig. 4: Fluorescence emission spectra of heme proteins in the presence of JGB. (A) Hb (3.5 µM) treated with 0, 2.24, 5.12, 9.6, 16.8, 18.08, 20.68 and 21.92 µM JGB (curves 1−8), (B) Mb (5 µM) treated with 0, 1.2, 4.8, 13.2, 20.4, 28.4, 31.2, 34 µM (curves 1−8).

Fig. 5: Stern-Volmer plot of heme proteins and JGB complexes at different temperature. Panel A and B represent Hb-JGB and Mb-JGB complexation data at temperature 285.15K (■), 298.15 K (●) and 308.15 K (▲).

Fig. 6: Synchronous fluorescence (Δλ = 15 and 60 nm) spectra of heme proteins in the presence of different concentrations of JGB. In panel A data of Hb (5 µM) at Δλ = 15 and (curves 1-9) denote JGB concentration in the range 0 to 35 µM and in panel B data of Hb (5 µM) at Δλ = 60 and curves (1-9) denote JGB concentration in the range 0 to 39 µM. In panel C data of Mb (5 µM) at Δλ = 15 and curves (1-9) denote JGB

Revised manuscript RA-ART-07-2014-006600

concentration in the range 0 to 33 µM and in panel D data of Mb (5 µM) at Δλ = 15 and curves (1-9) denote JGB concentration in the range 0 to 36 µM.

Fig. 7: Far UV and Soret band CD spectral changes of heme proteins. In panel A, curves (1−6) denote the spectral change of Hb (1 µM) in the presence of 0, 0.6, 4.8, 7.5, 14.4, 18 µM of JGB. In panel C curves (1−6) denote the spectral change of Mb (1 µM) in the presence of 0, 0.3, 2.1, 4.5, 8.1, 12.6 µM of JGB. In panel B, curves (1−6) denote the change of Soret band of Hb (5 µM) in the presence of 0, 1.2, 2.2, 4.2, 6.2, 8.2 µM of JGB. In panel D, curves (1−6) denote the change of Soret band of Mb (5 µM) in the presence of 0, 2.9, 6.2, 10.8, 14.1, 16.0 µM of JGB.

Fig. 8: Induced CD spectra of the heme proteins. JGB (30 µM) treated with 0, 10 , 15, 19, 23 and 30 µM of Hb (A) and Mb (B) as represented by curves (1-6).

Fig. 9: Three-dimensional fluorescence spectra and contour maps of Hb of 5 µM (A, B), Mb of 5 µM (C, D), 1:6 Hb–JGB complex (E, F) and 1:6 Mb-JGB complexes (G, H).

Fig.10: ITC profiles for the binding of heme proteins to JGB. The top panels (A) and (B) present raw results for the sequential titration of JGB (0.5 mM and 1 mM) into Hb (50 µM) and Mb (20 µM) solution, respectively, and dilution of JGB into buffer (curves on the top offset for clarity). The lower panels show the integrated heat results after correction of the heat of dilution against the mole ratio of JGB/heme proteins. The data points (closed squares) were fitted to a one-site model and the solid lines represent the best-fit result.

Fig. 11: Stern-Volmer plots of Hb-JGB and Mb-JGB complexes at different pH conditions. Panels A and B depict the Hb-JGB and Mb-JGB complexation at pH 6.4 (■), 7.4 (●), and 8.4 (▲).

Revised manuscript RA-ART-07-2014-006600

Fig. 12. CD and UV- melting profiles of Hb (A and B) and Mb (C and D). Curves (-■) and (-●-) represent pattern for the free protein and the protein complexed with JGB at a dye/heme protein molar reatio of 2.0.

Revised manuscript RA-ART-07-2014-006600

Table 1 Stern-Volmer quenching constant (K_{sv}), Lineweaver-Berk constant (K_{LB}), binding constant (K_b) and number of binding sites (n) for the interaction of JGB with Hb and Mb at different temperatures[a]

Protein	T/K	K_{sv}x10^4 /M^{-1}	K_{LB} x10^4 / M^{-1}	K_a x10^4 /M^{-1}	n
Hb	288.15	8.56	8.01	8.08	1.01
	298.15	6.59	6.80	6.82	1.07
	308.15	6.019	6.11	6.17	1.09
Mb	288.15	11.81	11.83	11.15	1.01
	298.15	8.61	8.87	8.51	1.10
	308.15	7.917	7.77	7.98	1.10

[a]The data presented are averages of four determinations.

Revised manuscript RA-ART-07-2014-006600

Table 2 Isothermal titration calorimetry data for the binding of JGB to Hb and Mb[a]

Protein	K x (10^4 M^{-1})	N	ΔG^0 (kcal/mol)	ΔH^0 (kcal/mol)	$T\Delta S^0$ (kcal/mol)
Hb	6.60	1.19	-6.61	15.13	21.74
Mb	8.21	1.10	-5.54	1.60	7.14

[a]All the data in this table are derived from ITC experiments at 298.15. K and ΔH^0 values were determined from ITC profiles by Origin 7.0 software. The values of ΔG^0 and $T\Delta S^0$ were determined as described in the text. All the ITC profiles were fit to a model of single binding sites.

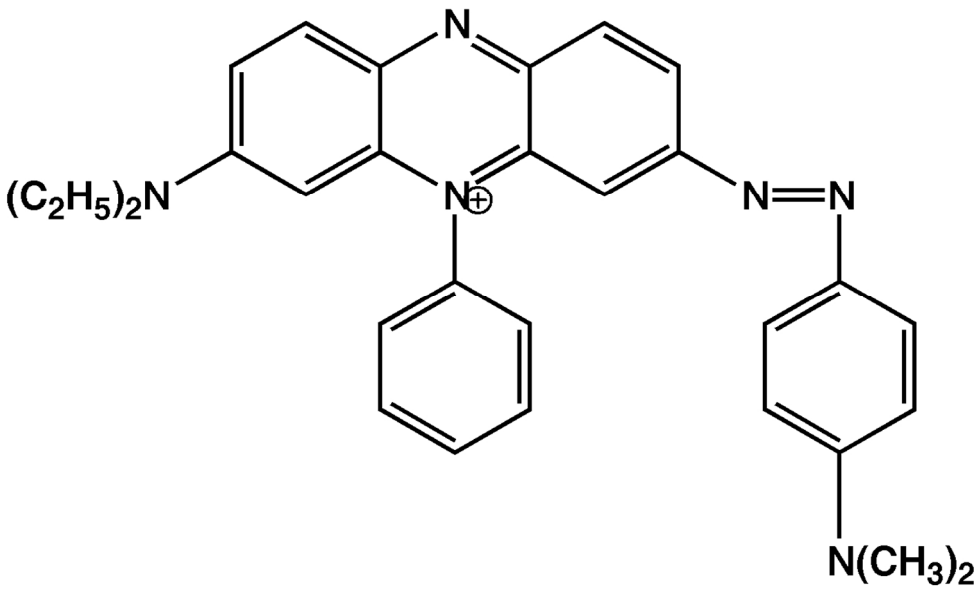

Chemical structure of janus green blue.
123x74mm (300 x 300 DPI)

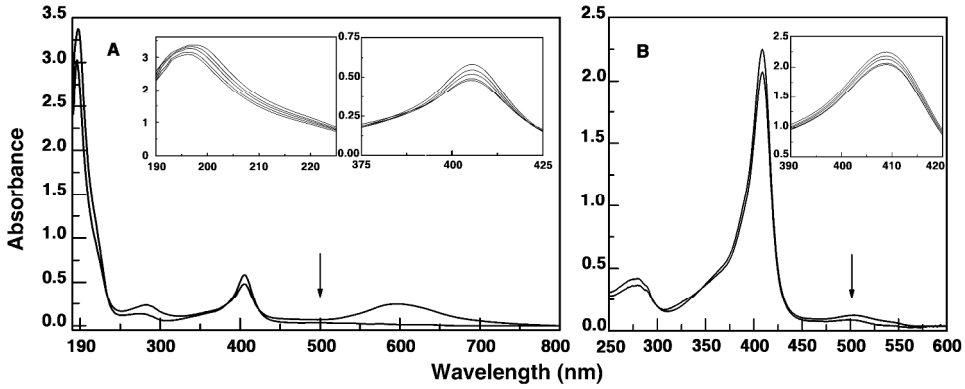

Absorption spectral changes of heme proteins in the presence of JGB. (A) Hb (3.5 μM) treated with 29 μM of JGB. (B) Mb (8 μM) treated with 60 μM of JGB. Inset: (A) 195 nm and 405 nm bands of Hb (3.5 μM) treated with 0, 2.56, 6.72, 17.6 and 29 μM (curves 1−5) of JGB and(B) 409 nm bands of Mb (8 μM) treated with 0, 6,17,43 and 60 μM (curves 1−5) of JGB are highlighted.
297x122mm (300 x 300 DPI)

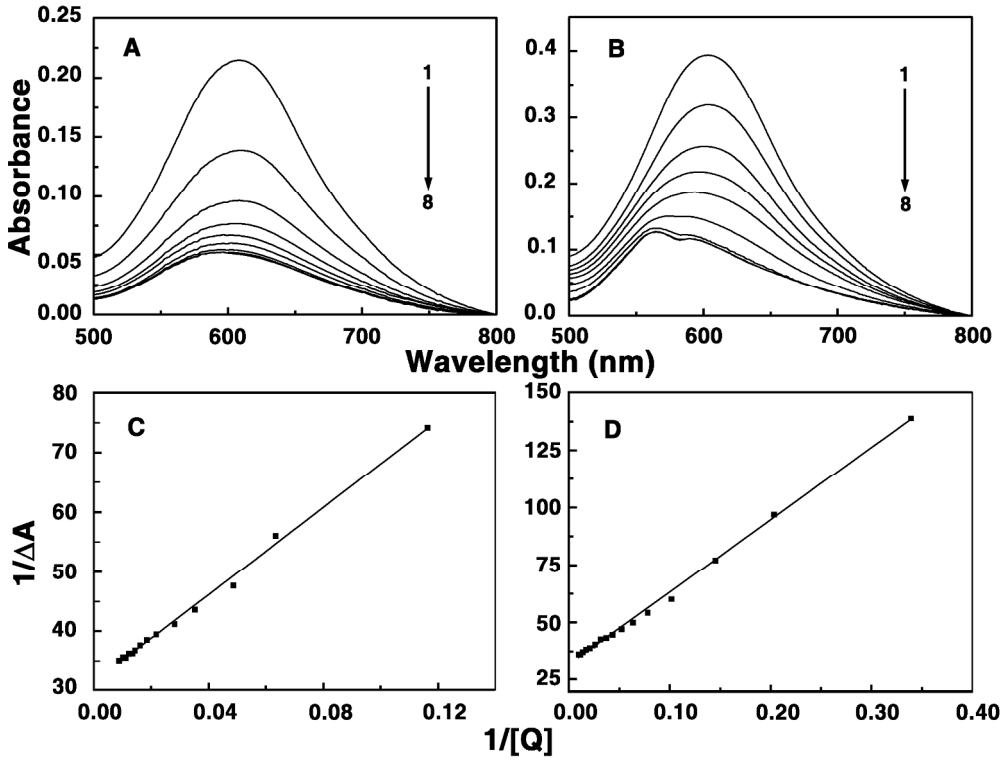

Absorption spectral changes of JGB in the presence and absence of the heme proteins. (A) JGB of 5.6 μM treated with 0, 0.7, 2.1, 3.5, 5.6, 7.7, 10.5, 12 and 14 μM of Hb (curves 1−9) and (B) JGB of 10.36 μM treated with 0, 2.9, 6.8, 9.8, 12.8, 22.8, 31.8, 58.8 and 65.8 μM of Mb (curves 1−9). (C) and (D) represent the Benesi-Hildebrand plots for the binding of JGB with Hb and Mb.
215x162mm (300 x 300 DPI)

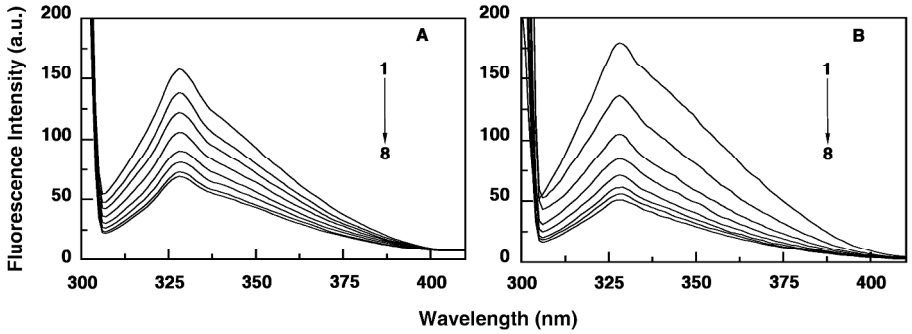

Fluorescence emission spectra of heme proteins in the presence of JGB. (A) Hb (3.5 μM) treated with 0, 2.24, 5.12, 9.6, 16.8, 18.08, 20.68 and 21.92 μM JGB (curves 1−8), (B) Mb (5 μM) treated with 0, 1.2, 4.8, 13.2, 20.4, 28.4, 31.2, 34 μM (curves 1−8).
285x104mm (300 x 300 DPI)

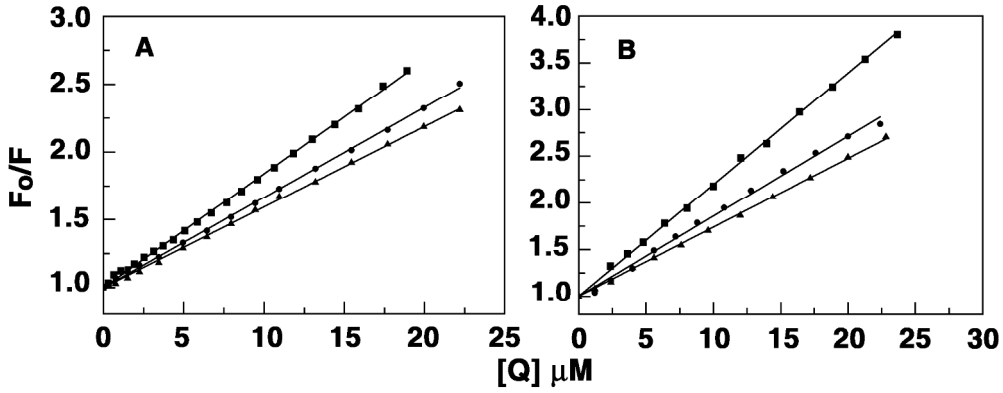

Stern-Volmer plot of heme proteins and JGB complexes at different temperature. Panel A and B represent Hb-JGB and Mb-JGB complexation data at temperature 285.15K (—), 298.15 K (□) and 308.15 K (▲).
214x86mm (300 x 300 DPI)

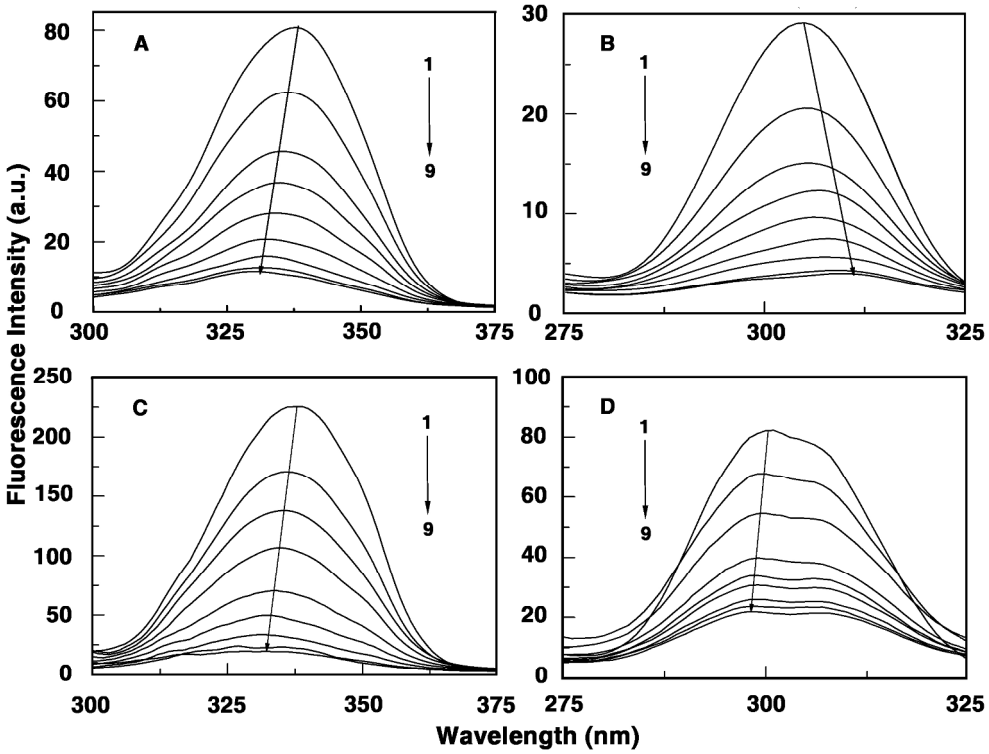

Synchronous fluorescence (Δλ = 15 and 60 nm) spectra of heme proteins in the presence of different concentrations of JGB. In panel A data of Hb (5 μM) at Δλ = 15 and (curves 1-9) denote JGB concentration in the range 0 to 35 μM and in panel B data of Hb (5 μM) at Δλ = 60 and curves (1-9) denote JGB concentration in the range 0 to 39 μM. In panel C data of Mb (5 μM) at Δλ = 15 and curves (1-9) denote JGB concentration in the range 0 to 33 μM and in panel D data of Mb (5 μM) at Δλ = 15 and curves (1-9) denote JGB concentration in the range 0 to 36 μM.
234x180mm (300 x 300 DPI)

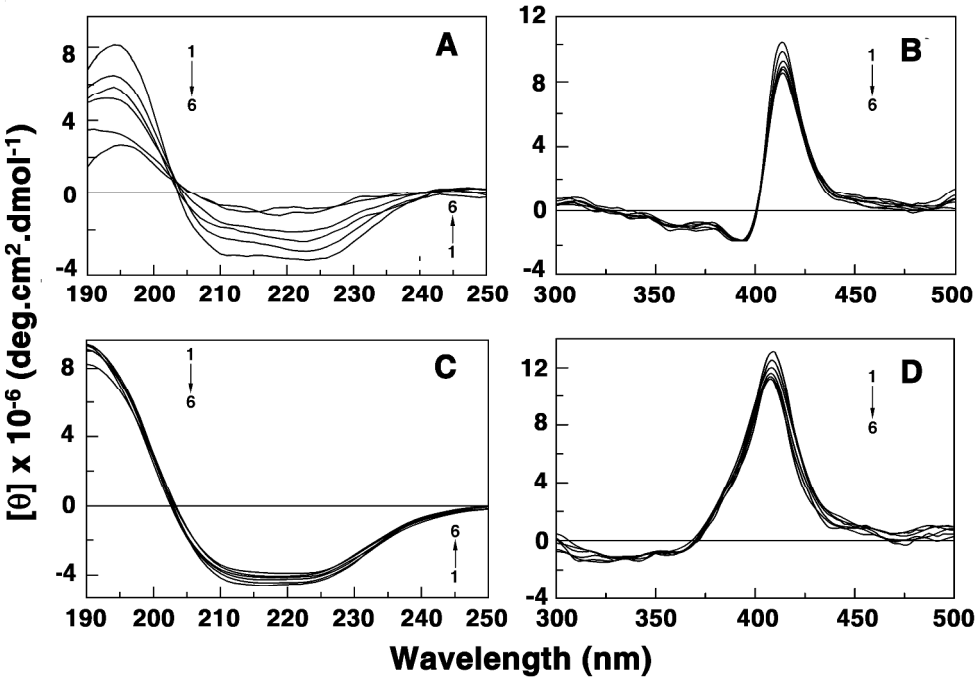

Far UV and Soret band CD spectral changes of heme proteins. In panel A, curves (1−6) denote the spectral change of Hb (1 μM) in the presence of 0, 0.6, 4.8, 7.5, 14.4, 18 μM of JGB. In panel C curves (1−6) denote the spectral change of Mb (1 μM) in the presence of 0, 0.3, 2.1, 4.5, 8.1, 12.6 μM of JGB. In panel B, curves (1−6) denote the change of Soret band of Hb (5 μM) in the presence of 0, 1.2, 2.2, 4.2, 6.2, 8.2 μM of JGB. In panel D, curves (1−6) denote the change of Soret band of Mb (5 μM) in the presence of 0, 2.9, 6.2, 10.8, 14.1, 16.0 μM of JGB.
295x202mm (300 x 300 DPI)

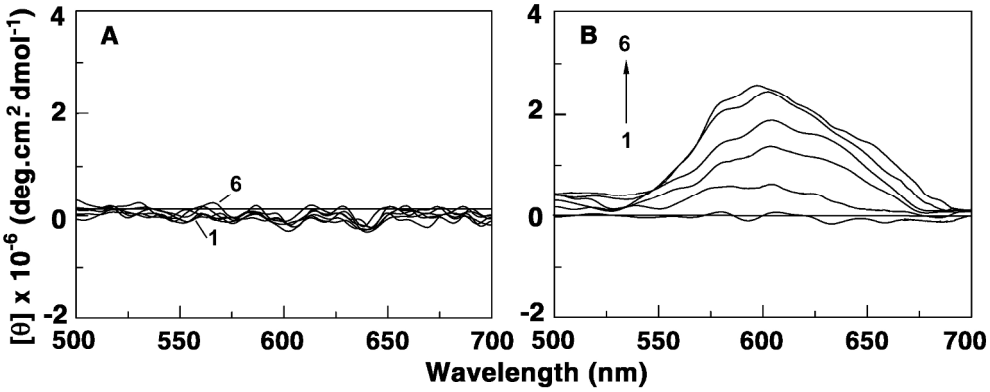

Induced CD spectra of the heme proteins. JGB (30 μM) treated with 0, 10 , 15, 19, 23 and 30 μM of Hb (A) and Mb (B) as represented by curves (1-6).
227x90mm (300 x 300 DPI)

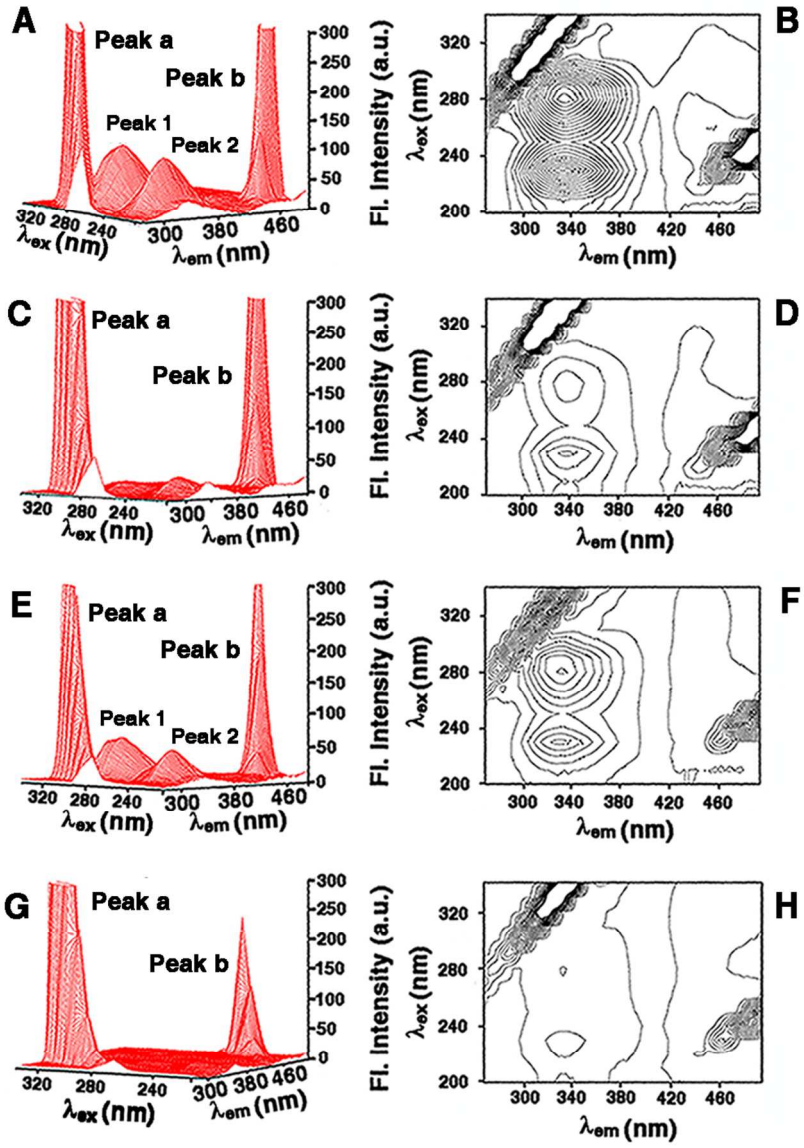

Three-dimensional fluorescence spectra and contour maps of Hb of 5 μM (A, B), Mb of 5 μM (C, D), 1:6 Hb–JGB complex (E, F) and 1:6 Mb-JGB complexes (G, H).
86x125mm (300 x 300 DPI)

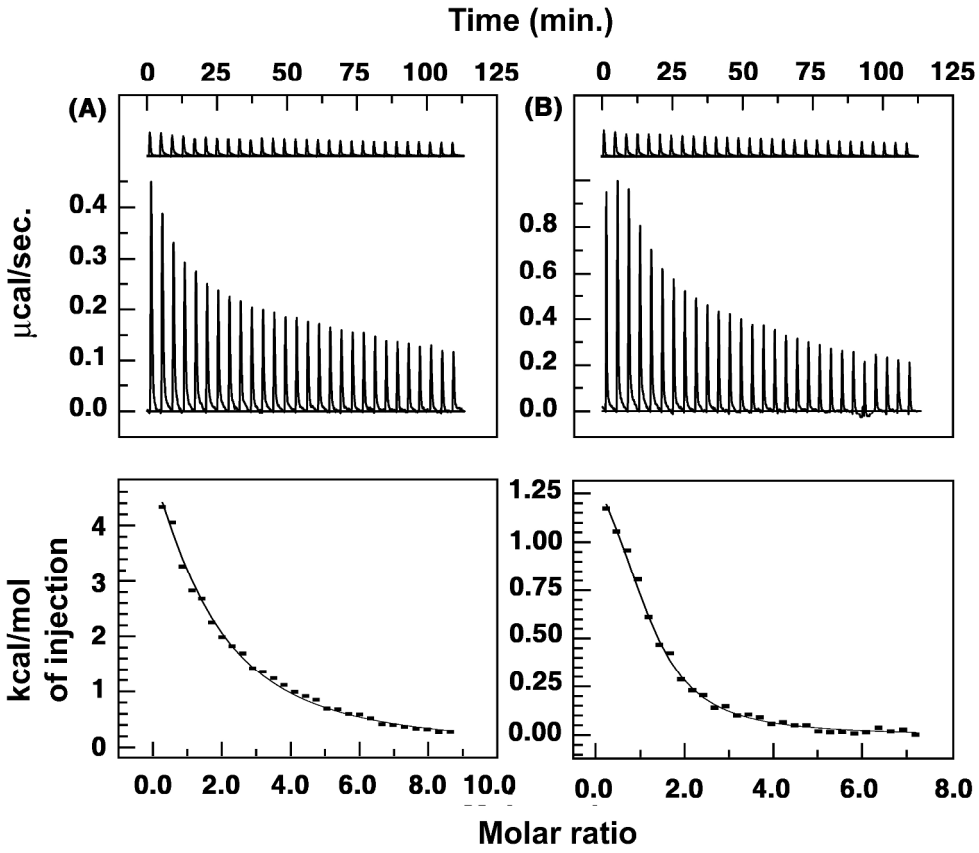

ITC profiles for the binding of heme proteins to JGB. The top panels (A) and (B) present raw results for the sequential titration of JGB (0.5 mM and 1 mM) into Hb (50 µM) and Mb (20 µM) solution, respectively, and dilution of JGB into buffer (curves on the top offset for clarity). The lower panels show the integrated heat results after correction of the heat of dilution against the mole ratio of JGB/heme proteins. The data points (closed squares) were fitted to a one-site model and the solid lines represent the best-fit result.
270x240mm (300 x 300 DPI)

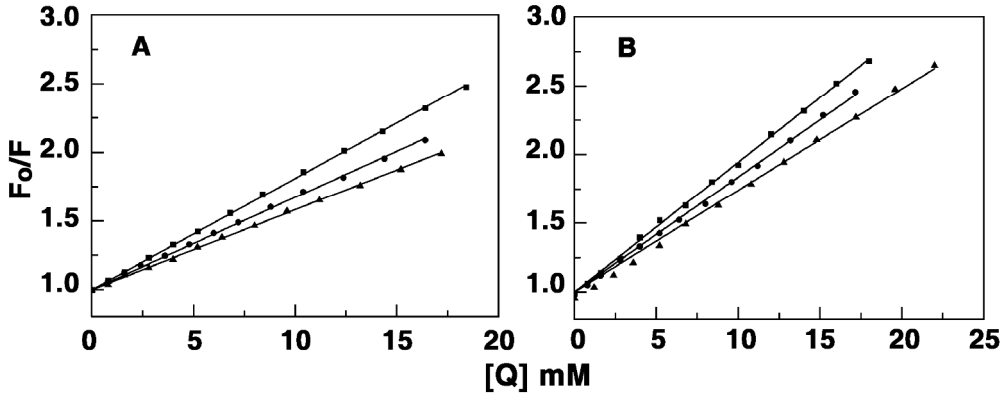

Stern-Volmer plots of Hb-JGB and Mb-JGB complexes at different pH conditions. Panels A and B depict the Hb-JGB and Mb-JGB complexation at pH 6.4 (—), 7.4 (□), and 8.4 (▲).
222x88mm (300 x 300 DPI)

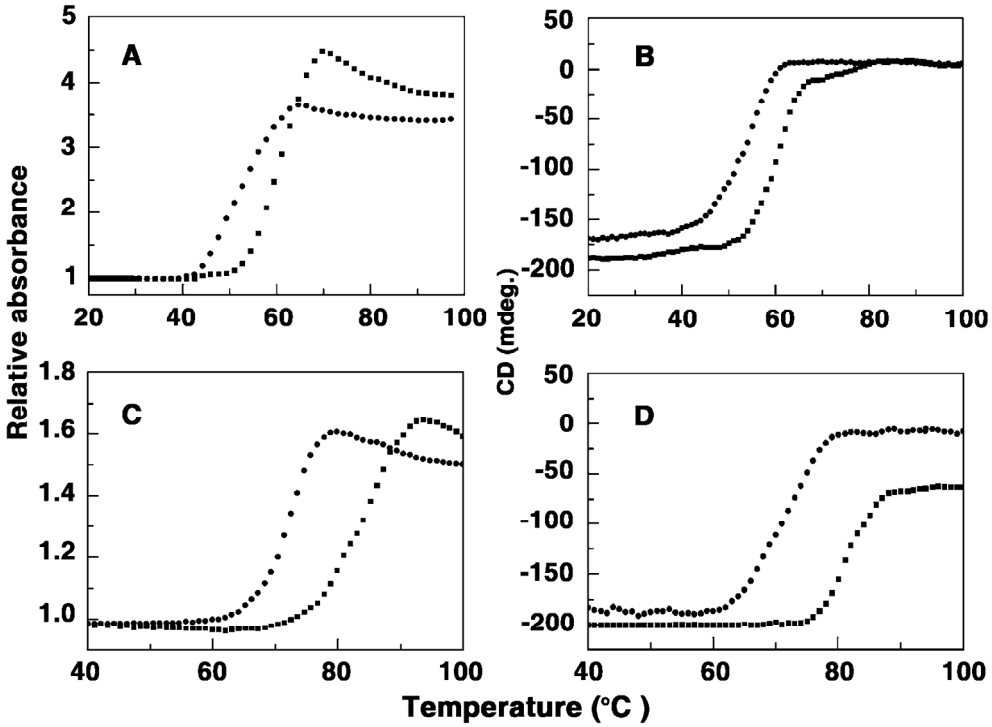

CD and UV- melting profiles of Hb (A and B) and Mb (C and D). Curves (-■) and (-●-) represent pattern for the free protein and the protein complexed with JGB at a dye/heme protein molar reatio of 2.0.
152x111mm (300 x 300 DPI)